Since January 2020 Elsevier has created a COVID-19 resource centre with free information in English and Mandarin on the novel coronavirus COVID-19. The COVID-19 resource centre is hosted on Elsevier Connect, the company's public news and information website.

Veterinary Microbiology, 20 (1989) 21–33
Elsevier Science Publishers B.V., Amsterdam — Printed in The Netherlands

Ultrastructure and Protein A–Gold Immunolabelling of HRT-18 Cells Infected with Turkey Enteric Coronavirus

S. DEA[1], S. GARZON[2], H. STRYKOWSKI[2] and P. TIJSSEN[1]*

[1]*Centre de Recherche en Médecine Comparée, Institut Armand-Frappier, Université du Québec, Laval-des-Rapides, Qué H7V 1B7 (Canada)*
[2]*Faculté de Médecine, Université de Montréal, Montréal, Qué H3C 3J7 (Canada)*

(Accepted for publication 21 November 1988)

ABSTRACT

Dea, S., Garzon, S., Strykowski, H. and Tijssen, P., 1989. Ultrastructure and protein A-gold immunolabelling of HRT-18 cells infected with turkey enteric coronavirus. *Vet Microbiol.*, 20: 21–33.

The Minnesota strain of turkey enteric coronavirus (TCV) was propagated in HRT-18 cells, a cell line derived from human rectum adenocarcinoma. A productive non-cytopathic infection was established, without a previous adaptation, in these cells as shown by the specific hemagglutinating activity in cell culture supernatants. A post-embedding immunochemical technique, using specific antiserum directed against the original egg-adapted virus and colloidal-gold-labelled protein A as the electron-dense marker, was used for the identification of the virus and related antigens in the cells by electron microscopy. Budding of typical coronavirus particles, through intracytoplasmic membranes and accumulation of complete virus within cytoplasmic vesicles or the lumen of rough endoplasmic reticulum, were the main features of the viral morphogenesis. Late in infection, numerous progeny viral particles were shown at the outer surface of infected cells, but budding could not be demonstrated at this level. Two different types of surface projections were observed on the extracellular particles of this avian coronavirus. These morphological characteristics have been thus far described only for mammalian hemagglutinating coronaviruses

INTRODUCTION

Transmissible enteritis (Bluecomb disease) of turkeys is an acute, highly infectious disease affecting turkeys of all ages, but especially poults <6 weeks of age (Pomeroy, 1984). Since the early 1970s, a coronavirus has been recognized as the primary etiological agent (Ritchie et al., 1973; King, 1975; Naqi et al., 1975). Turkey coronavirus (TCV) is propagated by oral inoculation of

*Author to whom correspondence should be addressed.

0378-1135/89/$03.50

1-day-old turkey poults or by inoculation into the amniotic cavity of embryonated turkey or chicken eggs with clarified intestinal contents from infected turkeys (Deshmukh et al, 1973; Naqi et al., 1975; Pomeroy, 1984). Despite numerous attempts, the original prototype Minnesota strain of TCV could not be cultivated in cell cultures of various origin including cultures of primary chicken and turkey embryonic cells (Deshmukh et al., 1973; King, 1975; Pomeroy, 1984). This has hampered the characterization of candidate TCV isolates and the development of practical and sensitive in vitro assays for the diagnosis of this viral infection.

Previously, we have shown that a few Quebec isolates of TCV can be propagated in primary chicken embryo kidney cell cultures and in HRT-18 cells, a cell line derived from human rectum adenocarcinoma (Tompkins et al., 1974), without inducing a distinct cellular degeneration (Dea et al., 1986). In this report, we describe the ultrastructure and the protein A–gold immunolabelling of TCV-infected HRT-18 cells. This immunocytochemical technique permitted both identification of the virus and related antigens, and investigation of some aspects of the viral morphogenesis.

MATERIALS AND METHODS

Source of virus

The prototype Minnesota strain of TCV (Ritchie et al., 1973) was kindly supplied to us by Dr. B.S. Pomeroy, College of Veterinary Medicine, St. Paul, MN, U.S.A. Viral stocks were prepared following two successive passages in 22 to 24-day-old embryonated turkey eggs and purified by differential and isopycnic centrifugation in sucrose gradients, as described previously (Dea et al., 1986).

Cell cultures

The human rectal tumor (HRT-18) cell line was obtained from Dr. J. Laporte, Institut de Recherche Agronomiques, Thiverval-Grignon, France. The cells were cultured in RPMI 1640 medium (Flow Laboratories) containing gentamycin (50 μg ml^{-1}), tylosin (60 μg ml^{-1}), lincomycin (25 μg ml^{-1}), fungizone (25 μg ml^{-1}) and 15% heat-inactivated fetal bovine serum (FBS). Confluent cell monolayers were maintained in RPMI containing 2% FBS.

Viral propagation

For viral propagation, HRT-18 cells were grown in 25- or 75-cm^2 Falcon plastic tissue culture flasks. Monolayers were rinsed twice with Dulbecco's phosphate-buffered saline (PBS) and then inoculated with 0.5 ml of various

dilutions of the clarified viral preparation. After 1.5 h of adsorption at room temperature, the inoculum was removed and replaced with 5 ml of maintenance medium without serum and adjusted to pH 8.0 with sodium bicarbonate. The cultures were incubated at 37°C, and checked daily for the presence of cytopathic changes. The subpassages were usually done at 5 to 6-day intervals. The cultures were harvested following two freeze–thaw cycles: the supernatant fluids were clarified by centrifugation at 5000× *g* for 30 min at 4°C and immediately tested for hemagglutinating (HA) activity using rat erythrocytes (Dea et al., 1986).

Antiserum

An anti-TCV hyperimmune serum was obtained after immunization of rabbits with the purified egg-adapted Minnesota strain. The specificity of the antiserum was confirmed by immunoelectron microscopy and hemagglutination inhibition (Dea and Tijssen, 1988).

Electron microscopy and protein A-gold immunolabelling

For transmission electron microscopy (EM), infected cell monolayers were fixed with 4% paraformaldehyde–0.5% glutaraldehyde in 0.1 M sodium phosphate buffer pH 7.4, for 30 min at room temperature, and treated for 1 h with 0.1 M NH_4Cl. After washing with PBS supplemented with 4.5% sucrose (w/v), the cells were scraped free from the flasks with a rubber policeman, transferred into a centrifuge tube, and spun down at 800× *g* for 10 min at 4°C. The pellets were then dispersed in 0.1 ml of 2% low-melting agarose (Seaplaque Agarose, FMC Corporation, Rockland, MD, U.S.A.) and the cells were spun down again by low-speed centrifugation. After gelification, cellular pellets were cut into small blocks (1 mm^3) with a razor blade, dehydrated in graded ethanol and embedded in Araldite 502. Thin sections (70–90 nm thick) were mounted on 400-mesh naked-nickel grids and processed for immunocytochemical labelling using colloidal gold as a marker (Garzon et al., 1982). The grids were first floated for 5 min on a drop of TBS (0.05 M Tris–HCl, 0.15 M NaCl, pH 8.0) containing 0.05% Tween 20, and then incubated for 60 min at room temperature on a drop of a 200-fold dilution of the rabbit anti-TCV hyperimmune serum in TBS–Tween. After washing in TBS–Tween, grids were incubated on a drop of TBS-diluted protein A–gold (PAG) complex. The colloidal gold particles in the PAG complex were 8 nm in diameter and were prepared according to the method described by Frens (1973), with the modifications suggested by de Mey (1983). The sections were finally washed with TBS, rinsed in distilled water and counterstained with uranyl acetate and lead citrate (Fracca and Parks, 1965). Microscopic examination was performed on an EM300 Philips microscope. The specificity of the labelling was demonstrated

by controls including non-immune sera, incubation with PAG complex alone and incubation with non-infected cells.

RESULTS

Significant cytopathic changes were observed neither during nor after five weekly blind passages of TCV in HRT-18 cells using conventional cultivation procedures. A few rounded, enlarged and refractile cells, that progressively tended to aggregate into small clumps, were the only features observed during the course of infection. The evidence of viral replication in these cells included the observation of typical coronavirus particles by EM, and the demonstration of a weak HA activity (titers ranging from 1/16 to 1/32) in the supernatant culture fluids from each of the first five passages. The HA activity could be inhibited by pre-incubation of the supernatants with the rabbit anti-TCV hyperimmune serum. An intense immunogold labelling of coronavirus particles,

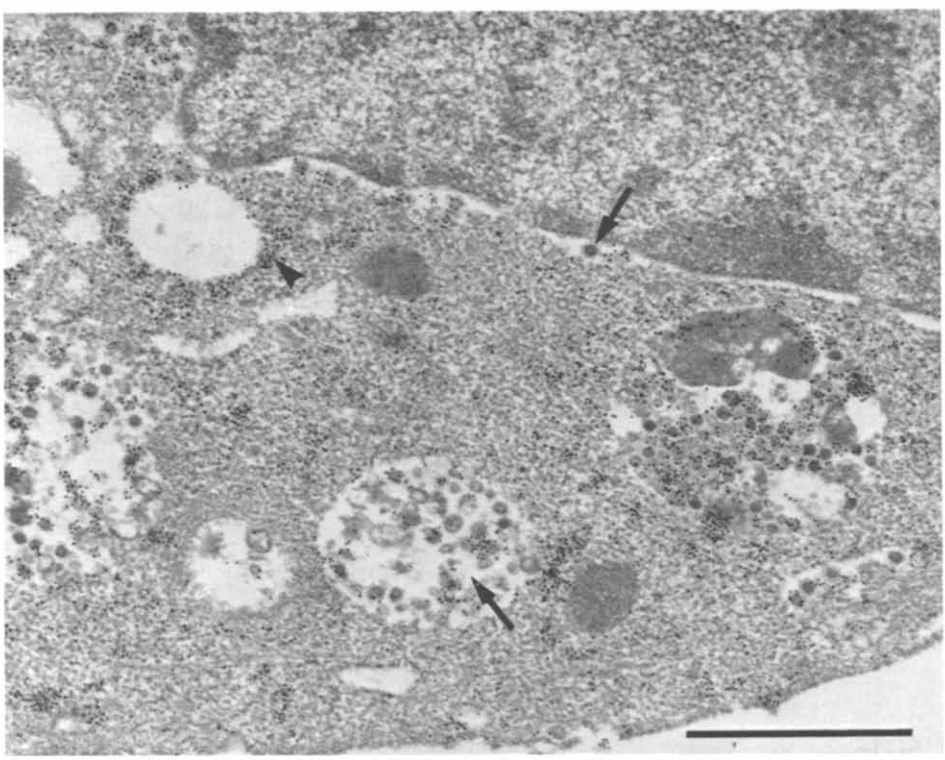

Fig 1. Immunogold labelling of the TCV virions located in the intracellular vesicles and in the lumen of the nuclear envelope (arrows). By 10–12 h after infection, the viral antigens detected by the PAG complex tended also to cluster around empty vacuoles (arrowhead). The bar represents 2 μm

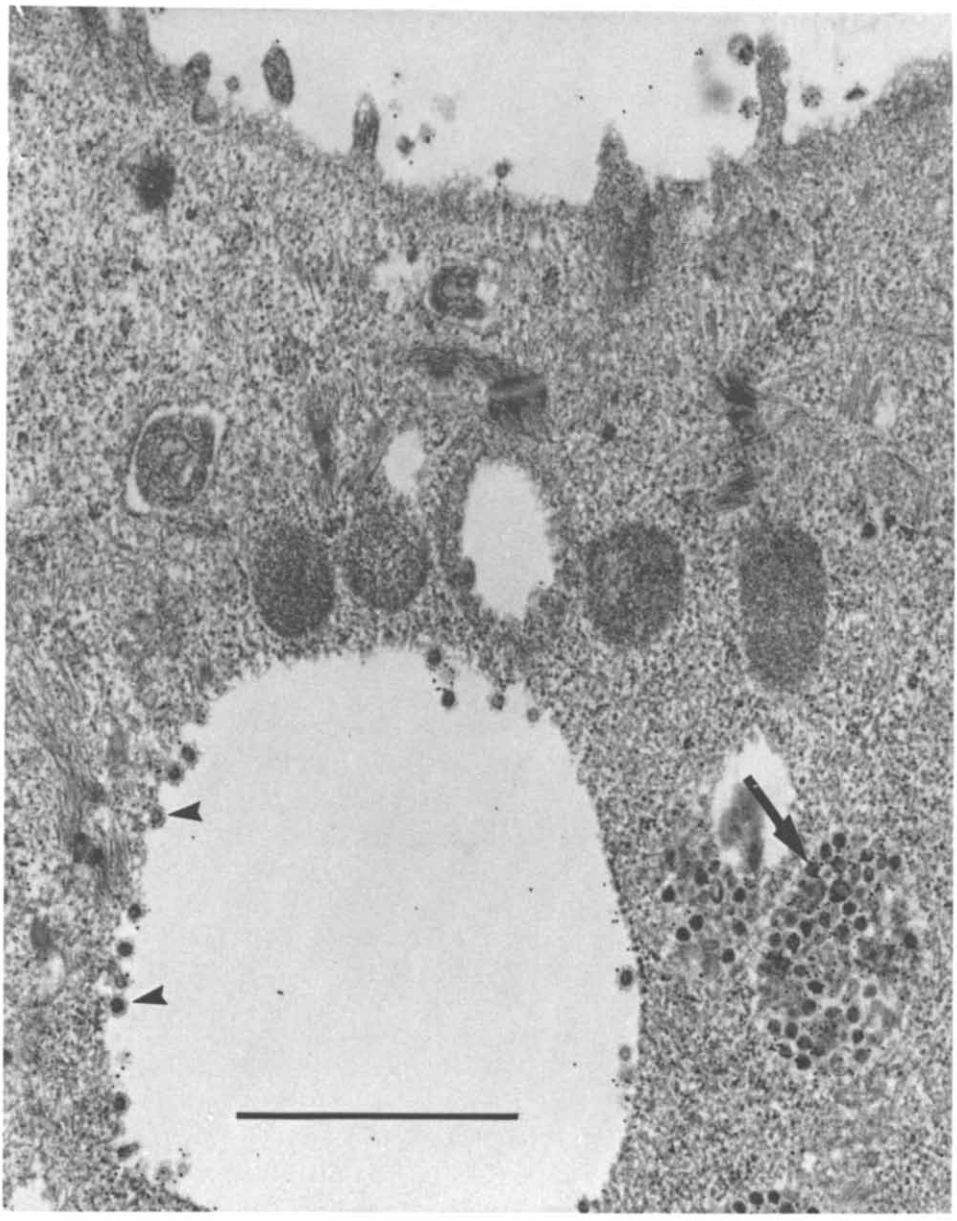

Fig. 2. Immunogold labelling of nascent TCV particles budding from the membrane of smooth-walled vesicles (arrowheads) and accumulation of the progeny particles in these intracytoplasmic vacuoles (arrows). The bar represents 2 μm.

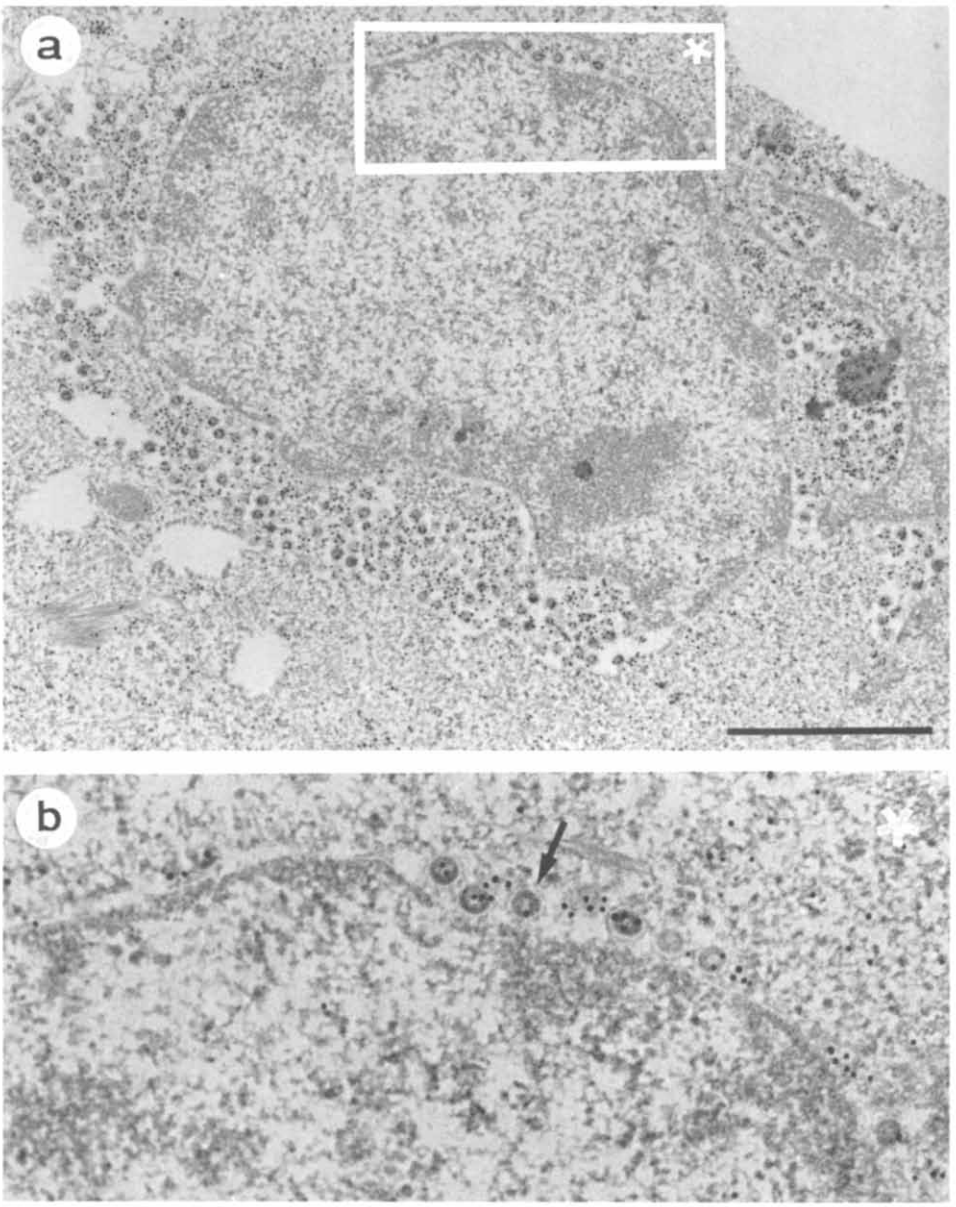

Fig. 3. (a) Large numbers of immunolabelled virions present in the lumen of the rough endoplasmic reticulum surrounding the nucleus. The virions appear as spherical particles with electron-lucent or dense centers and possess spiky or bulbous surface projections (arrow). The fuzzy coat next to the inner side of the viral envelope probably represents the viral nucleocapsid (b) Higher magnification (3×) of viral particles in outlined area of (a). The bar represents 2 μm

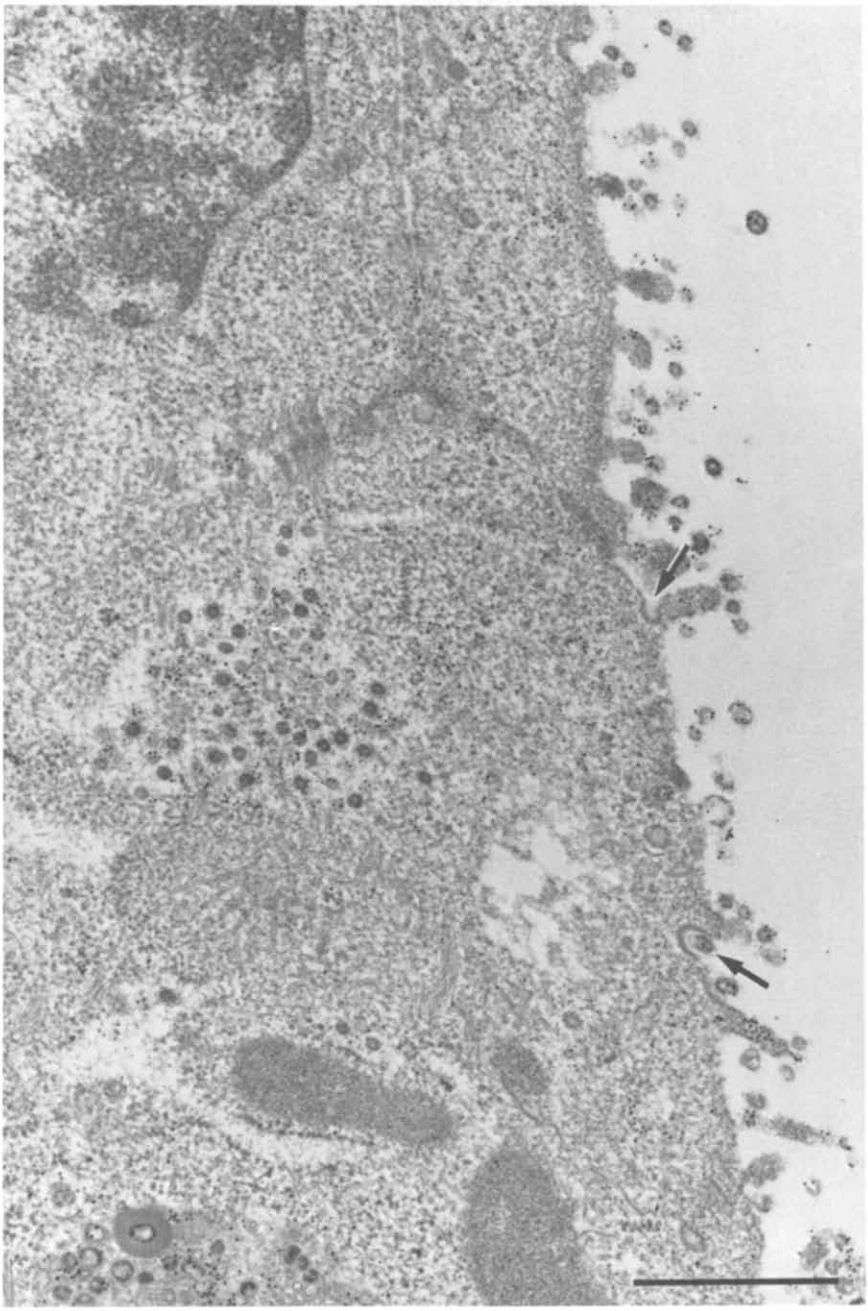

Fig 4. By 18–24 h after inoculation, progeny particles were labelled at the outer surface of infected cells and in the lumen of small vesicles migrating to the cell surface. The arrows indicate exocytotic or endocytotic vesicles surrounding extracellular virions. The bar represents 1 μm

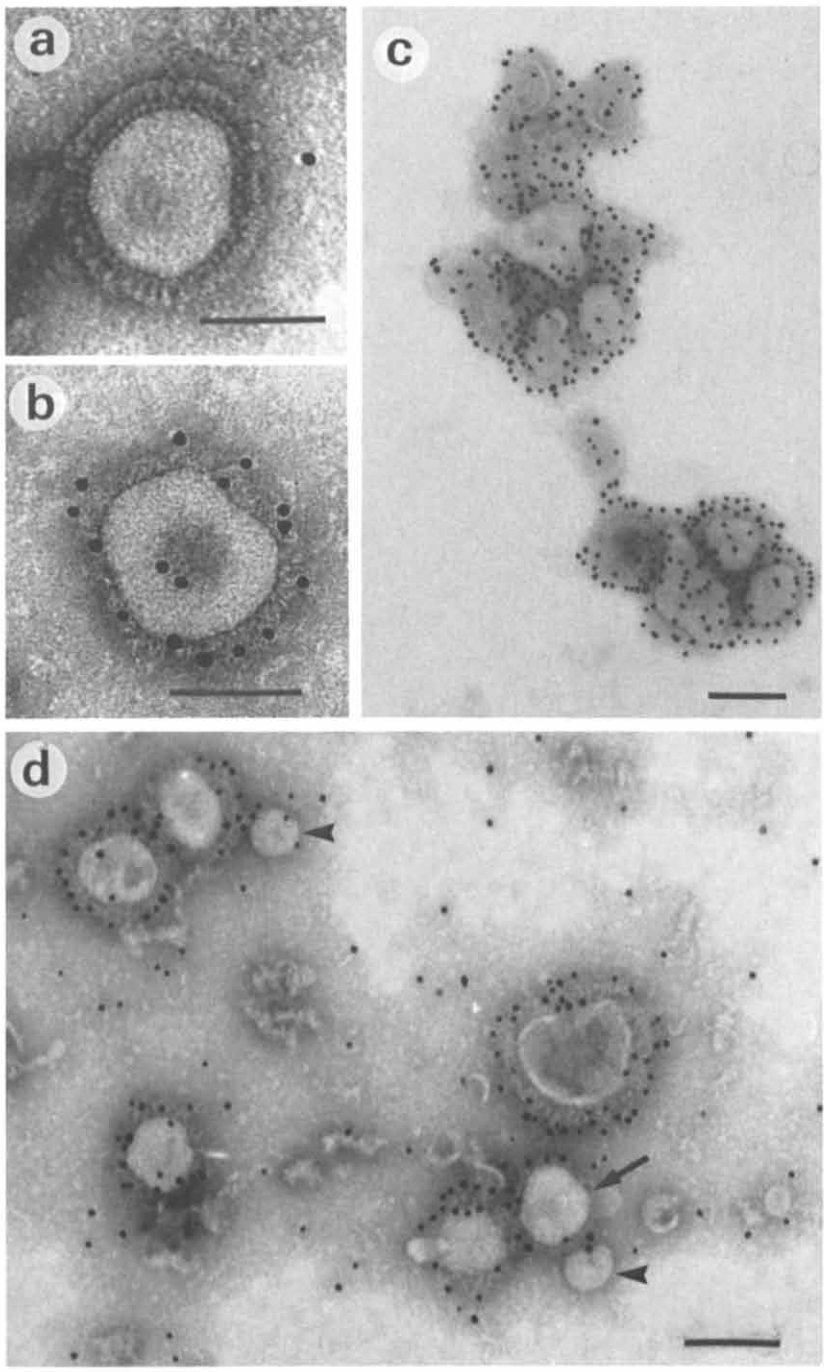
a
b
c
d

located in the cytoplasmic vesicles of infected cells, was observed by EM at 12 and 18 h after infection (Fig. 1). Uninfected HRT-18 cells treated in the same way, with the same antiserum, as well as infected-cell cultures incubated with the pre-immune serum or buffer prior to the protein A–gold treatment, showed no significant labelling, thus confirming the specificity of the reaction.

Differences in labelling densities among the intracellular compartments were observed at various times after inoculation. Immunodetection of the virus in these cells showed gold complexes largely dispersed in the cytosol, after 6–8 h of incubation. By 10–12 h after infection, the PAG-labelled antigens tended to accumulate in more specific regions of the cytosol, particularly around intracytoplasmic vesicles (Fig. 1). Budding of viral particles through intracytoplasmic membranes could be detected by immunolabelling as soon as 8 h after infection (Fig. 2). This was followed rapidly by an accumulation of viral particles within intracellular vacuoles. The virions were also commonly seen in the lumen of the nuclear envelope (Fig. 1), but at no time was labelling observed in the nuclear region. Occasionally, large numbers of labelled virions were found in the area immediately surrounding the nucleus, possibly corresponding to the lumen of the rough endoplasmic reticulum (Fig. 3a). The intracellular virions appeared as spherical particles with electron-lucent or -dense centers, and as having spiky or bulbous peplomers in their envelope (Fig. 3b).

By 18–24 h after infection, progeny particles could be detected at the outer surface of infected cells, but the virions did not seem to be released from the cell by budding since no gold labelling was observed on the plasma membrane itself (Fig. 4). Instead, the virions appeared to exit within vesicles that migrate to the cell membrane and fuse with it. Small vesicles containing labelled viral particles were commonly observed near the cell surface and, in a few instances, exocytotic vesicles were shown partly surrounding extracellular virions. Later, large aggregates of progeny viral particles were detected near the outer surface of infected cells (data not shown). During the course of TCV infection, only mild structural changes were induced in the infected cells and viral particles were only occasionally observed in the intercellular spaces.

The extracellular viral particles were enveloped, moderately pleomorphic, but mostly spherical in shape, and averaged 120 nm in diameter (Fig. 5). The peplomers formed a fringe radiating from the viral envelope and they appeared to be club-shaped, 15–20 nm in length. Additional small granular projections

Fig 5 Immunogold labelling of extracellular TCV particles: (a) An unlabelled viral particle, as observed following incubation with pre-immune serum, which shows a double fringe of surface projections; (b) immunogold labelling of an individual viral particle after incubation with rabbit anti-TCV hyperimmune serum; (c) two rows of gold granules were frequently demonstrated around extracellular virions; (d) the gold granules were located near the tips of the surface peplomers. Note the absence of labelling around viral particles without surface projections (arrowheads). The arrow indicates a viral particle that lost only the large peplomers, but still possesses the fringe of small granular projections The bars represent 100 nm

located near the base of the peplomers were also observed on the viral particles following incubation with the rabbit pre-immune sera (Fig. 5a). The fringe of small granular projections appeared to be masked, probably by immunoglobulins, following the incubation with the rabbit anti-TCV hyperimmune sera (Fig. 5b). Two rows of gold granules were frequently present at the surface of immunolabelled viral particles (Fig. 5c). The gold granules were generally located near the tip of both types of surface projections, whereas the interior of the virus was not labelled. Only a few gold granules were observed around viral particles that lost their surface projections (Fig. 5d). This suggests that the polyclonal anti-TCV hyperimmune serum contained mainly antibodies to the antigenic determinants situated at the surface of the virions.

DISCUSSION

The present report focused on ultrastructural observations of the replication of turkey enteric coronavirus in an established cell line originated from a human rectal adenocarcinoma. In these cells, the virus rapidly established a productive infection without previous adaptation and without obvious cytopathic effect. Virus replication was initially suggested by direct EM of supernatant fluids and by the demonstration of a specific cell-free HA activity (Dea et al., 1986). The post-embedding protein A–gold immunocytochemical approach was used for the identification and localization of virus (antigens) produced in TCV-infected HRT-18 cells. A specific antiserum, obtained after immunization of rabbits with the purified egg-adapted Minnesota strain of TCV, was used as the immunoreactant. The strong positive reaction observed in TCV-infected cells and the absence of labelling in the various controls confirmed that the virus which replicated in HRT-18 cells was identical to the original virus cultivated in embryonated turkey eggs.

The use of colloidal gold as an electron-dense marker allowed for easy identification of the maturing virions. Although the various events of the viral morphogenesis were not investigated in detail in this study, absence of viral antigens in the nucleus, budding and accumulation of progeny virus particles in the lumina of cytoplasmic cisternae, transport through smooth-walled intracellular vesicles, and absence of viral budding at the surface of the cells are all features shared with other members of the Coronaviridae family (Doughri et al., 1976; Siddell et al., 1982; Dubois-Dalcq et al., 1985), including the avian infectious bronchitis (IBV) virus (Nazerian and Cunningham, 1968; Chasey and Alexander, 1976). The results of the present study also suggest that the progeny TCV particles are released from the cells, by a mechanism involving the cellular secretory apparatus. Such a mechanism has also been suggested in cases of mouse hepatitis virus (Sturman and Holmes, 1983; Tooze and Tooze, 1985) and for IBV (Chasey and Alexander, 1976).

Our observation of two different types of surface projections on the extra-

cellular viral particles agree with the morphological features that have been thus far described only for mammalian hemagglutinating coronaviruses, namely the porcine hemagglutinating encephalomyelitis virus (Callebaut and Pensaert, 1980), the bovine enteric coronavirus (King et al., 1985), the coronavirus DVIM of mice (Sugiyama and Amano, 1980) and the human respiratory coronavirus OC43 (Hogue and Brian, 1986). However, the presence of additional granular projections has not been described for IBV, although the virus possesses a hemagglutinating activity (Berry et al., 1964; Biswal et al., 1966; Bingham and Almeida, 1977). This major morphological difference between these two unrelated avian coronaviruses has not been mentioned in previous descriptions of the bluecomb virus (Panigraphy et al., 1973; Naqi et al., 1975).

This study also provides the first evidence on the replication and the propagation of an avian coronavirus in cell cultures derived from human tissues, or in mammalian cell cultures, without previous adaptation. HRT-18 cells have been previously reported to be susceptible to enteropathogenic strains of bovine (Laporte et al., 1980; King et al., 1985; Reynolds et al., 1985), canine and human coronaviruses (Laporte et al., 1980; Hogue et al., 1984). The high tropism of these viruses for mature enterocytes has been demonstrated by in vivo and in vitro studies (Doughri et al., 1976; Sturman and Holmes, 1983; Pomeroy, 1984; Dubois-Dalcq et al., 1985). The susceptibility of the transformed cell line to these viruses may be related to the fact that it has maintained many characteristics of the normal mature enterocytes, particularly the presence of microvilli on which the viral receptors are probably located (Tompkins et al., 1974). Another possibility would be that HRT-18 cells have receptors for both calf and turkey coronaviruses as a result of oncogenic transformation. Further work is needed to understand this particular tropism of TCV and its significance in the biology and epidemiology of the virus. As previously suggested for bovine coronavirus (Hogue et al., 1984), the possibility of a human infection by TCV cannot be excluded.

The post-embedding immunogold labelling technique has been shown to be of particular relevance to the temporal localization of structural and non-structural viral proteins in virus-infected cells (Bendayan, 1984). We are currently producing monoclonal antibodies directed against the various viral polypeptides with the aim of obtaining more information on the in vivo process of TCV multiplication.

ACKNOWLEDGEMENTS

We would like to acknowledge the skilled technical assistance of J. Beaubien. The authors also thank Dr. Claude Montpetit for his help in obtaining HRT-18 cells. This work was supported by the Conseil des recherches et services agricoles du Québec and the Quebec Federation of Poultry Producers. Serge

Dea has received a Fellowship from the Medical Research Council of Canada and has submitted this work as part of a Ph.D. thesis.

REFERENCES

Bendayan, M., 1984. Protein A-gold electron microscopic immunocytochemistry. methods, applications, and limitations. J. Electron Microsc Tech , 1 243-270.

Berry, D M , Cruickshank, J.G., Chu, H P. and Wells, R.J.H., 1964. The structure of infectious bronchitis virus. Virology, 23 403-407.

Bingham, R W and Almeida, J.D , 1977. Studies on the structure of a coronavirus avian infectious bronchitis virus J Gen. Virol , 36· 495-502.

Biswal, R W , Nazerian, K. and Cunningham, C.H., 1966 A hemagglutinating fraction of infectious bronchitis virus Am. J Vet. Res., 27. 1157-1167.

Callebaut, P.E and Pensaert, M B , 1980 Characterization and isolation of structural polypeptides in haemagglutinating encephalomyelitis virus J Gen Virol , 48 193-204

Chasey, D and Alexander, D.J , 1976. Morphogenesis of avian infectious bronchitis virus in primary chick kidney cells. Arch Virol., 52: 101-111

Dea, S. and Tijssen, P , 1988. Identification of the structural proteins of turkey enteric coronavirus. Arch Virol , 99: 173-186

Dea, S., Marsolais, G , Beaubien, J and Ruppanner, R , 1986. Coronaviruses associated with outbreaks of transmissible enteritis (Bluecomb) of turkeys in Quebec· hemagglutination properties and cell cultivation Avian Dis., 30: 319-326

De Mey, J , 1983. Colloidal gold probes in immunocytochemistry. In. J Polack and S. van Noorden (Editors), Immunocytochemistry: Applications in Pathology and Biology. J. Wright, London, pp. 82-113.

Deshmukh, D.R., Larsen, C T and Pomeroy, B.S., 1973. Survival of Bluecomb agent in embryonating turkey eggs and cell cultures Am. J Vet. Res., 34: 151-161

Doughri, A M., Storz, J., Hajer, I. and Fernando, H.S , 1976. Morphology and morphogenesis of a coronavirus infecting intestinal epithelial cells of new born calves. Exp. Mol. Pathol , 25 355-370.

Dubois-Dalcq, M E , Holmes, K.V. and Rentier, B , (Editors), 1985. Assembly of Enveloped RNA Viruses (Coronaviridae). Springer, Wein/New York, pp 110-120.

Fracca, J M. and Parks, V.R , 1965. A routine technique for double-staining ultrathin sections using uranyl and lead salts. J. Cell Biol., 25: 151-161.

Frens, G., 1973 Controlled nucleation for the regulation of the particle size in monodisperse gold solutions. Nat. Phys Sci , 241: 20-22

Garzon, S , Bendayan, M and Kurstak, E., 1982. Ultra-structural localization of viral antigens using the protein A-gold technique J. Virol. Meth , 5. 67-73

Hogue, B G and Brian, D A., 1986 Structural proteins of human respiratory coronavirus OC43. Virus Res , 5 131-144

Hogue, B.G., King, B and Brian, D.A., 1984 Antigenic relationships among proteins of bovine coronavirus, human respiratory coronavirus OC43, and mouse hepatitis coronavirus A59. J Virology, 51. 384-388.

King, D.J., 1975 Comments on the etiology and immunity of transmissible (coronaviral) enteritis of turkey (Bluecomb). Am. J. Vet. Res , 38· 555-556

King, B , Potts, B J and Brian, D.A , 1985. Bovine coronavirus hemagglutinin protein. Virus Res., 2 53-59

Laporte, J , Bobulesco, P and Rossi, F., 1980. Une lignée particulièrement sensible à la réplication du coronavirus entérique bovin. les cellules HRT-18. C R Acad. Sci Paris, t. 290D 623-626.

Naqi, S.A., Panigraphy, B. and Hall, C.F., 1975. Purification and concentration of viruses associated with transmissible (coronaviral) enteritis of turkeys (Bluecomb). Am. J. Vet. Res., 36 548-552

Nazerian, B. and Cunningham, C.H., 1968 Morphogenesis of avian infectious bronchitis virus in chicken embryo fibroblasts J Gen. Virol., 3: 469-470.

Panigraphy, B., Naqi, S.A. and Hall, C.F., 1973. Isolation and chacterization of viruses associated with transmissible enteritis (Bluecomb) of turkeys. Avian Dis., 17: 430-438.

Pomeroy, B.S., 1984. Coronaviral enteritis of turkeys. In: M.S. Holstad, H.J Barnes, B W Calnek, W M Reid and H.W. Yoder (Editors), Diseases of Poultry, 8th edn. Iowa State University Press, Ames, pp. 553-559.

Reynolds, D.J., Debney, T.J., Hall, G A , Thomas, L.H. and Parsons, K R , 1985. Studies on the relationship between coronaviruses from the intestinal and respiratory tracts of calves. Arch. Virol., 85: 71-83.

Ritchie, A.E., Deshmukh, D.R., Larsen, C.T. and Pomeroy, B.S , 1973. Electron microscopy of coronavirus-like particles characteristic of turkey Bluecomb disease. Avian Dis , 17: 546-558.

Siddell, S T., Wege, H. and Ter Meulen, V., 1982. The structure and replication of coronaviruses. Curr. Top. Microbiol. Immunol., 99: 131-163

Sturman, L S and Holmes, K.V., 1983 The molecular biology of coronaviruses. Adv Virus Res., 28· 35-112.

Sugiyama, K. and Amano, Y , 1980. Hemagglutination and structural polypeptides of a new coronavirus associated with diarrhea in infant mice. Arch. Virol., 66· 95-105

Tompkins, W.A.F., Watrach, A.W., Schmale, J.D., Schultz, R.M. and Harris, J.A., 1974. Cultural and antigenic properties of newly established cell strains derived from adenocarcinomas of the human colon and rectum. J. Natl. Cancer Inst., 52· 101-106.

Tooze, J. and Tooze, S A , 1985. Infection of AtT20 murine pituitary-tumour cells by mouse hepatitis virus strain A59: virus budding is restricted to the Golgi region. Eur J. Cell Biol , 37 203-212.